TORQUE PULSATION STUDY FROM DESIGN SIDE

A. B. Asaf ali

1 INTRODUCTION

For the poly phase permanent magnet synchronous (PPSM) machine, torque ripple results from magneto motive force (MMF) set up by the armature current harmonics and the reluctance variations due to the slot openings in the stator. Under load torque oscillation is also caused by the interaction of magnets with the space harmonics generated by the spatial distribution of the MMF. In applications for example, where a low speed drive is preferred, torque ripple is an important criterion in order to reduce vibrations and to have low acoustic noise. In this report various steps to reduce the torque ripple from the design side will be discussed.

2 CALCULATION METHODS

In general, the force or torque of electrical machines can be calculated from current sheet distribution and flux density distribution. For PPSM, the calculation method is based on current sheet of stator winding and magnets. The research will be concentrated later in solving the field equation as in many cases the expected results can be obtained in less time than with FEM. The force exerted on a conductor is calculated using Lorentz equation as

$$\vec{F} = q\left(\vec{E} + \vec{\upsilon} \times \vec{B}\right) \tag{2.1}$$

The sum of tangential components created by electric field strength is zero and it does not contribute. Fields in the airgap are of interest and can be solved for given boundary conditions. The analytical model equation is provided in [1]. This complicated field equation has not been used at this stage, but the results have been provided based on FEM. The fields in other regions cause secondary effects. For such solutions an idealized model is chosen in which the slot is replaced by smooth surface and the current carrying windings are replaced by fictitious infinitely thin current sheet. For sinusoidal space and time varying field the force density is given by the equation

$$\tau_w = \frac{\hat{A}_{s1} \cdot \hat{B}_{\delta 1}}{2} \cdot \cos(\alpha) \tag{2.2}$$

where $\hat{A}_{s1}$ and $\hat{B}_{\delta 1}$ are fundamental components of current sheet and no-load flux density.

The other methods that are often used in FEM calculations are Maxwell stress tensor and virtual work method. For example in Maxwell stress tensor the stresses are divided into tangential and normal with respect to the volume under consideration. The volume force density can be written as divergence of tensor *T*

$$\tau_V = \nabla \cdot T \tag{2.3}$$

$$T = \frac{1}{\mu_0}\begin{pmatrix} B_x^2 - \frac{1}{2}|B|^2 & B_x B_y & B_x B_z \\ B_y B_x & B_y^2 - \frac{1}{2}|B|^2 & B_y B_z \\ B_z B_x & B_z B_y & B_z^2 - \frac{1}{2}|B|^2 \end{pmatrix} \tag{2.4}$$

The total force can be obtained by integrating over the volume. Using vector divergence theorem, the volume integral can be transformed into a surface integral. Thus the tangential and normal stresses for two dimensional unit depth are

$$\tau_{Ft} = \frac{B_n B_t}{\mu_0} \qquad \tau_{Fn} = \frac{B_n^2 B_t^2}{2\mu_0} \tag{2.5}$$

For the force calculation Lorentz equation is still applicable and is explained in the next section.

2.1 Stator current sheet harmonics and slot harmonics

Each machine type has its own current sheet distribution. Each slot loading will generate its own amplitude for certain time. The arbitrary current sheet is shown in **figure 1** below.

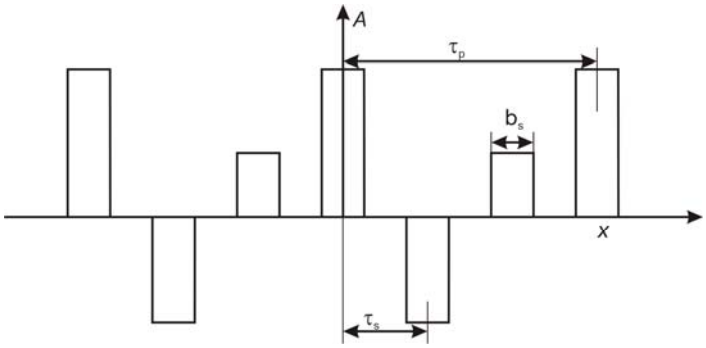

Figure 1: Arbitrary current sheet

The current sheet in Fourier series can be expressed as

$$A_k(x) = \sum_{k=1}^{m} \sum_{\nu=1}^{\infty} i_k \cdot c_{k\nu} \cdot \cos\left(\frac{\pi\nu}{\tau_p} x - \varphi_{k\nu}\right) \tag{2.6}$$

$$c_{k\nu} = \sqrt{a_{k\nu}^2 + b_{k\nu}^2}$$

$$\varphi_{k\nu} = \tan^{-1}\left(\frac{b_{k\nu}^2}{a_{k\nu}^2}\right)$$

where i_k is the current in the slot. The effect of space harmonics is included in the above equation. The harmonics travel in either direction proportional to reciprocal of their order with or against the fundamental wave. These calculations can be easily made with help of software tools. For m phases of stator winding the order of harmonics can be expressed as

$$\upsilon = (2mN \pm 1) \quad , \tag{2.7}$$

where N is a positive integer. For the integer slot winding arrangement the harmonics exist only with odd numbers, but in fractional slot winding topology even order harmonics and sub-harmonics may appear [2]. For concentrated winding with double layer winding arrangement the order of harmonics can be expressed as

$$\upsilon' = \frac{\upsilon}{p^*} \quad , \tag{2.8}$$

where p^* is the number of poles in the required base winding [2, 3]. The winding arrangements and the winding factors of concentrated winding are not discussed here. Slot harmonics due to slotting of stator are also present in both integer slot windings and concentrated windings arrangement. Its harmonics is of the form

$$\upsilon_{slot} = (2mqN \pm 1) \quad , \tag{2.9}$$

where N is a positive integer and q is the number of slots per pole per phase. In general, the harmonics represent with the assumptions made that each particular set of space harmonics exists in a separate machine and those individual machines of similar type have to be interconnected as there are space harmonics present. Harmonics may be deemed as produced by sets of additional poles superimposed on the fundamental poles.

The following **figure 2** shows the current sheet distribution and the Fourier synthesis of 2/3 arrangement of concentrated type. The ordinal number of current sheet always occurs in pairs and they have the same amplitude. These are due to slot harmonics. For winding type of 2/3 topology **figure 2** shows that the fundamental component of current sheet is the torque producing component.

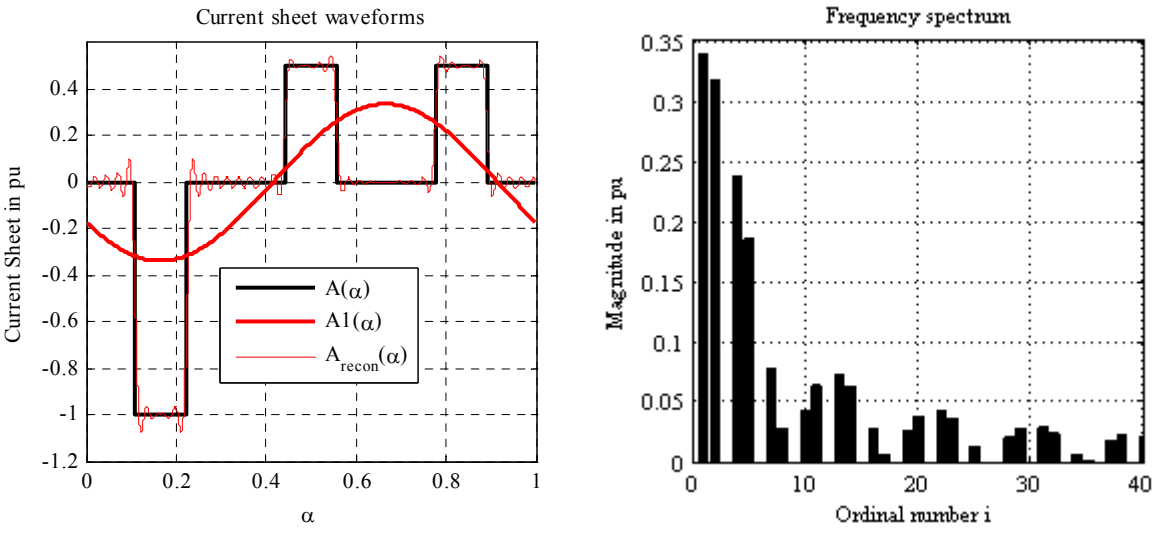

Figure 2: Current sheet and its harmonics for 2/3 topology PPSM

In some cases the current sheet is treated as ratio of current over slot pitch. However the amplitude of the fundamental component remains the same. It can also be assumed to have an infinitesimal slot opening width and assume the wave to travel around the span of coil. In

such a case MMF distribution is obtained by integrating the current sheet. The MMF distribution is $\pi/2$ electrically phase shifted from current sheet. The comparison between MMF and current sheet distribution were made in [4]. If the winding is not skewed, the assumption has been made that the current in the *z* direction is constant and the slot current density varies only in the *x* direction. At any position *x* in the airgap the differential current is

$$\frac{dI(x)}{dx} = A_s(x) \cdot \tau_p \tag{2.10}$$

where A_s is the current sheet. If the no-load airgap flux density $\hat{B}_\delta$ and the current I are perpendicular to each other then according to the Lorentz law the force is

$$F = A_s(x) \cdot \tau_p \cdot x \cdot B(x) \cdot l_{Fe} \tag{2.11}$$

where l_{Fe} is the iron length of the machine. Torque can be obtained when this equation is multiplied with the radius of the machine. This result is similar to the tangential stress in the equation (2.2).

2.1 Airgap flux density

The no-load airgap flux density is from permanent magnets of the rotor. It is expressed as

$$B(x,t) = \sum_{\nu=1}^{\infty} \hat{B}_\nu \cos\left(\frac{\pi\nu}{\tau_p} x - \omega t\right) \tag{2.12}$$

A typical no-load flux density distribution and its harmonics for surface mounted PPSM calculated from FEM simulation [5] is shown in **figure 3** below.

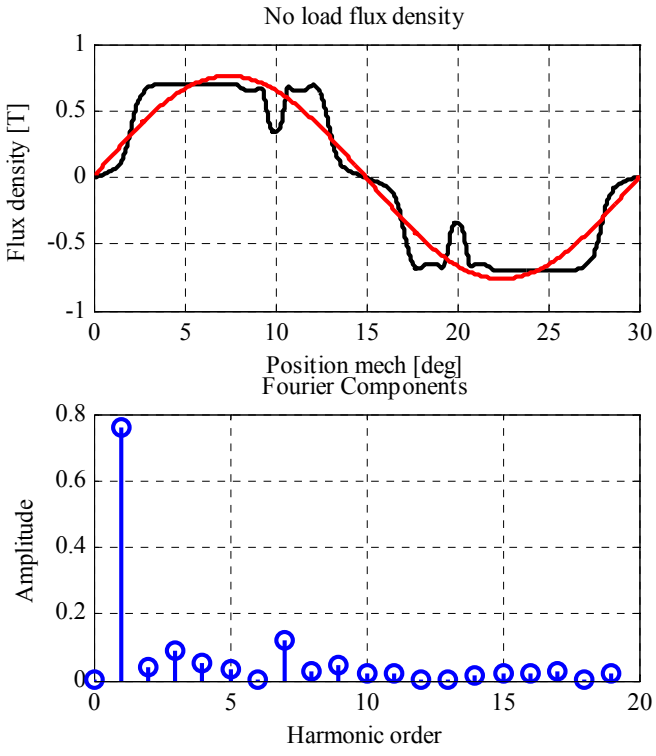

Figure 3: No-load flux density and its harmonics

In the **figure 3** the no-load flux density is considered for one period and its corresponding fundamental wave distribution is also shown. The no-load flux density has dips caused by stator slots, which creates losses on the rotor surface. It can be minimized by examining the stator slot opening, its shape and shape of the waveform too. Thus from the above discussion the harmonics of both stator and rotor field interact and produce torque pulsations.

3 INFLUENCE OF PARAMETERS

There are two kinds of torque pulsations in PPSM: Cogging torque exists under no-load conditions and torque ripple exists under load conditions. The methods used to minimize the torque ripple with and without load are varying the magnet strength and magnetization direction [6], varying the relative magnet width for different values of q (slots per pole per phase) [7], introducing auxiliary teeth and slots [7], varying slot opening and ratio of pole-arc to pole-pitch. The torque ripple can also be reduced if skewing is employed. In this work the influence of slot opening and ratio of pole-arc to pole-pitch are shown. For the analysis of the torque pulsations constraints have to be made by keeping certain parameters as constant. The volume of the magnet is maintained same for all calculations. The stator diameter and inner rotor diameter are kept same and the current density is also same for all calculations. The basic investigations are explained in the sections below for the geometry shown in the **figure 4** below.

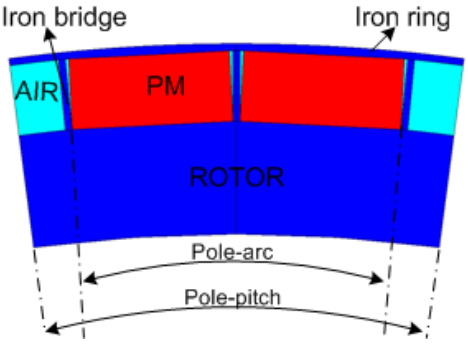

Figure 4: Geometry of the rotor with two magnets for one pole

This type of arrangement is called protected magnet type. With only a thin iron layer on top of the magnets, the protected magnets may be considered as surface mounted with almost no saliency [8]. For the investigations below the related values of torque ripple are defined as the peak to peak value of torque ripple to the percentage of the rated torque (3 kN). The same applies for the relative cogging torque calculations. It can be expressed as

$$M_{\%,i} = \left(\frac{M_{\Delta}}{M_N} \right) \cdot 100 \quad , \tag{3.1}$$

where i belongs either to cogging or ripple, M_{Δ} is the peak to peak value and M_N is the rated torque.

3.1 Influence of slot opening and ratio of pole-arc to pole-pitch at no-load

The effect of ratio of pole-arc to pole-pitch and the effect of slot opening width calculated from FEM (Flux [5]) is shown in **figure 5**. The variation of slot opening is from 3 mm to 7 mm. The pole-arc to pole-pitch ratio is varied from 0.53 to 0.9. **Figure 5** shows the variation of $M_{\%,cogging}$ for the considered geometry. From FEM simulations the minimum cogging torque can be obtained at a pole-arc to pole-pitch ratio of 0.7 and a slot opening of 3 mm. The cogging torque could be completely eliminated if there is no slot opening.

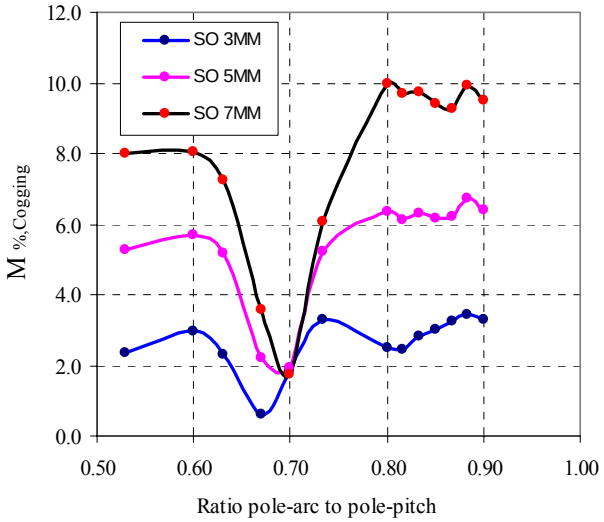

Figure 5: Cogging torque by varying parameters

3.2 Influence of slot opening and ratio of pole-arc to pole-pitch at load

The calculated value $M_{\%,ripple}$ of torque ripple with load current is shown in **Figure 6** for different ratio of pole-arc to pole-pitch for the considered geometry. The torque ripple and cogging torque have different minima for the same ratio of pole-arc to pole-pitch. This is mainly due to the saturation of the teeth edges.

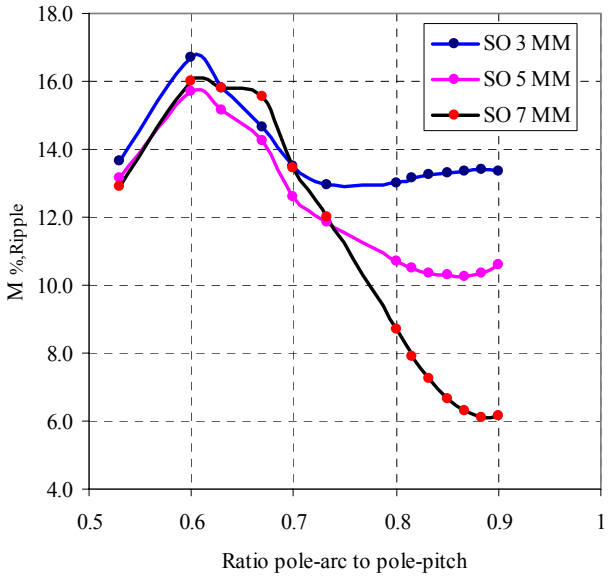

Figure 6: Torque ripple by varying parameters

In the previous section the current sheet discussion is based on the assumption that their fields are on the surface of the stator air-gap neglecting its saturation, leakage and slotting effect (smooth air-gap model). In reality the secondary effects of fields in the iron region causes unsymmetrical saturation. For example the iron region between the magnet and rotor surface shifts the minimum point of torque ripple. With slot opening of 3 mm the minimum point is at ratio 0.82. For slot opening of 5 mm the minimum point moves to 0.85. This minimum point for torque ripple calculation differs from minimum point of cogging torque calculation.

4 SUMMARY

In this report methods to minimize torque oscillation by varying design parameters are shown. The design optimization parameters are slot opening and pole-arc to pole-pitch. For the analysis constraints have been made to parameters like magnet mass and current density. The model discussed here is an arrangement with almost no saliency. There are alternative methods to reduce the torque pulsations such as skewing but these methods are not considered.

REFERENCE

[1] H. Mosebach: *Einfache analytische Rechenmodelle für permanentmagneterregte Synchronmaschinen*,
Electrical Engineering, Archiv für Elektrotechnik, Vol. 81 (1998), Heft 3, pp. 171-176

[2] J. Pyrhönen, T. Jokinen, V. Hrabovcova: *Design of Rotating Electrical Machines*,
John Wiley & Sons, Ltd, first edition 2008, ISBN 978-0-470-69516-6

[3] K. Vogt: *Berechnung Elektrischer Maschinen*,
VCH Verlagsgesellschaft mbH Weinheim, 1996, ISBN 3-527-28391-9

[4] D. Gerling: *Analysis of the Magnetomotive Force of a Three-Phase Winding with Concentrated Coils and Different Symmetry Features*,
IEEE Transactions on Magnetics, Vol. 39, No.5, September 2003

[5] FLUX 2D, Cedrat, Version 10.3

[6] T. Tudorache, L. Melcescu, M. Popescu, M. Cistelecan: *Finite Element Analysis of Cogging Torque in Low Speed Permanent Magnet Wind Generators*,
ICREPQ 2008, Santander, Spain

[7] Z. Q. Zhu, S. Ruangsinchaiwanich, N. Schofield, D. Howe: *Reduction of Cogging Torque in Interior-Magnet Brushless Machines*,
IEEE Transactions on Magnetics, Vol. 39, No.5, September 2003

[8] W.-R. Canders, A. B. Asaf ali: *Torque Ripple Situation in High Torque Synchronous Machine with Protected Magnets*,
ISEF 2009, Arras, France